Automated Cobb Angle Measurement at Scale: Identifying Undiagnosed Scoliosis in the UK Biobank

Authors

Marili Niglas[1]*, Brandon Whitcher[1], Marjola Thanaj[1], Nicolas Basty[1], Camilo Bell-Bradford[1], Liliana Szabo[1,2], E Louise Thomas[1], Jimmy D Bell[1]

Affiliations

[1] Research Centre for Optimal Health, School of Life Sciences, University of Westminster, London, United Kingdom

[2] William Harvey Research Institute, NIHR Barts Biomedical Research Centre, Queen Mary University of London, Charterhouse Square, London, United Kingdom

* Corresponding author: m.niglas@westminster.ac.uk

Funding

This research was funded by a Calico Life Sciences LLC research grant.

Disclosure

None of the authors has a conflict of interest to disclose.

Author contributions

M.N.: Data curation, Formal analysis, Investigation, Methodology, Software, Validation, Visualization, Writing - original draft, Writing - review & editing. B.W.: Conceptualization, Data curation, Formal analysis, Methodology, Software, Supervision, Writing - review & editing. M.T.: Data curation, Investigation, Writing - review & editing. N.B.: Conceptualization, Data curation, Investigation, Methodology, Writing - review & editing. C.B.B.: Data curation; Validation, Writing - review & editing. L.S.: Conceptualization, Investigation, Methodology, Writing - review & editing. E.L.T.: Conceptualization, Supervision, Writing - review & editing. J.D.B.: Conceptualization, Project administration, Supervision, Writing - review & editing.

Acknowledgements

The authors would like to thank Frances Williams for input on the manuscript. We would also like to thank the participants in the UK Biobank imaging study. This research was carried out using the UK Biobank Application number 44584, and funded by a Calico Life Sciences LLC research grant.

Abstract

Background context

Adult degenerative scoliosis develops after skeletal maturity in a previously normal spine, often as a result of age-related spinal degeneration, with its prevalence increasing due to longer life expectancy. Structural changes such as disc degeneration, osteoporosis, and measures of muscle quality can contribute to spinal instability. The Cobb angle is the standard method for quantifying spinal curvature severity, calculated as the angle between the most tilted vertebrae.

Purpose

To derive automated Cobb angle measurements from chemical-shift-based water-fat separation (Dixon) magnetic resonance images (MRI) and investigate associations with

anthropometric, socioeconomic variables, health conditions including back pain, and other image-derived phenotypes related to body composition.

Design

Cross-sectional study.

Patient sample

Participants from the UK Biobank study having abdominal MRI scans from the first imaging visit (n = 33,889).

Outcome measures

The maximal Cobb angle was automatically derived from vertebral bone marrow segmentation via a centroid-based spline-fitting method.

Methods

We measured the Cobb angle from MRI scans using a deep learning algorithm for vertebral bone marrow compartment labelling, followed by spline fitting over these labels. We compared scoliosis prevalence based on both self-reported as well as clinically diagnosed scoliosis and MRI-derived Cobb angle defined scoliosis. Additionally, we explored sex-specific relationships between Cobb angle and anthropometric variables, body composition measurements, and health conditions using correlation and linear regression models

Results

From a cohort of 33,889 UK Biobank participants, scoliosis was formally diagnosed or self-reported in a total of 170 subjects (0.5%), whereas 9,497 participants (28%) were identified on abdominal MRI via the algorithm as having some form of scoliosis based on a Cobb angle >10°. Among participants without a formal diagnosis of scoliosis, but identified by the algorithm, the majority (95.4%) were categorised as having mild scoliosis (< 25°). Compared to males, female participants had a higher mean Cobb angle (9.02 ± 5.59° vs 8.44 ± 4.79°, respectively), were more likely to have scoliosis, and exhibited higher Cobb angles across all age groups ($p < 0.000549$, Bonferroni-corrected). Linear regression analysis revealed significant associations between Cobb angle and age (β = 0.12 [0.11, 0.13] for female, β = 0.09 [0.08, 0.10] for male), paraspinal muscle fat infiltration (β = 0.08 [0.07, 0.08] for female, β = 0.05 [0.04, 0.06] for male), chronic back pain (β = 0.07 [0.04, 0.09] for female, β = 0.05 [0.02, 0.07] for male), and visceral adipose tissue (β = -0.06 [-0.08, -0.05] for female, β = -

0.06 [-0.07, -0.05] for male). Additionally, iliopsoas muscle volume was significantly negatively associated with Cobb angle in male participants only (β = -0.02 [-0.03, -0.01], $p < 0.000549$). However, the sex-stratified models showed low R^2 values, indicating that other unmeasured factors substantially contribute to the observed variation.

Conclusions

These findings suggest that a significant portion of the UK population has scoliosis that remains undiagnosed clinically, the majority of whom have a mild form of scoliosis. Our results are consistent with previous studies showing a higher prevalence of scoliosis in females as well as highlighting the association between spinal curvature, paraspinal muscle quality, and chronic back pain regardless of gender, osteoporosis or age.

Keywords

Scoliosis, magnetic resonance imaging, artificial intelligence, UK Biobank, Cobb angle, back pain

Abbreviations

ASAT	Abdominal subcutaneous adipose tissue
BMD	Bone mineral density
CT	Computer tomography
ICD	International Classification of Diseases
IDP	Image-derived phenotype
MET	Metabolically equivalent task
MRI	Magnetic resonance imaging
PDFF	Proton density fat fraction
SD	Standard deviation
T2D	Type two diabetes
VAT	Visceral adipose tissue
VBM	Vertebrae bone marrow

Introduction

Scoliosis is a condition characterised by an abnormal lateral curvature of the spine. It can be categorised into non-idiopathic scoliosis types such as musculoskeletal, neuromuscular or congenital scoliosis. However, the most common form is idiopathic scoliosis, which is primarily diagnosed in adolescence. In adults, scoliosis can be divided into two main types: residual adolescent idiopathic scoliosis, which persists into adulthood and de novo degenerative scoliosis, which develops later in life due to ageing and spinal degeneration.

Adult degenerative scoliosis is a form of scoliosis that develops after skeletal maturity in a previously normal spine [1]. With increasing life expectancy and age-related spinal degeneration, the prevalence of degenerative scoliosis is rising, along with patient expectations for correction to address cosmetic, functional, and pain-related concerns [2]. The condition arises from several factors, including asymmetric degeneration of intervertebral discs and facet joints, along with the breakdown of the extracellular matrix. These structural changes are worsened by processes like inflammation and abnormal blood vessel growth, which further damage disc tissues [3]. Additionally, conditions such as osteoporosis and sarcopenia, as well as injuries like vertebral fractures, contribute to spinal instability by weakening the bones and muscles around the spinal column [4]. Together, these factors lead to an uneven distribution of biomechanical stress on the spine, accelerating scoliosis progression.

The prevalence of primary degenerative scoliosis among adults varies significantly, with estimates ranging from 2% to 68%, and a pooled prevalence of 38% for adult-onset scoliosis, according to a recent systematic review and meta-analysis [5]. The condition is more commonly reported in females than males, and its prevalence is notably higher in individuals over 60 compared to younger adults. While the majority of patients do not experience symptoms, the primary symptoms are progressively worsening chronic back pain and neurogenic claudication, which eventually may lead to functional loss, such as leg weakening [1]. While radiographic diagnosis of scoliosis could provide more accurate prevalence estimates, large-scale studies to support this analysis were limited until recently.

The gold standard method for diagnosing scoliosis is from standing spinal radiographic images, which provide a clear view of the vertebral endplates used to calculate the Cobb angle [6]. Other diagnostic techniques to visualise the spinal column, such as computed tomography (CT), ultrasound, or magnetic resonance imaging (MRI) have been used for scoliosis screening [7,8]. From these medical images, the angle formed between the superior endplate of the most tilted vertebra and the inferior endplate of the lowest tilted

vertebra is defined as the Cobb angle. Scoliosis is diagnosed if the angle exceeds 10°, and can further be categorised according to the magnitude of the angle for progression [1,9,10]. The severity of spinal deformation guides clinicians in treatment planning and assists in selecting patients who may need closer monitoring for progression. For example, a Cobb angle above 30° in participants aged 48 years and older has been identified as a risk factor for an accelerated rate of spinal curvature progression [11,12].

Traditionally, the Cobb angle is calculated manually from the medical images, yet this method is subject to variability [13,14]. As such, multiple automated methods have been developed to assist radiographers in improving time-efficiency and intra- and inter-rater readability, which is particularly crucial for scoliosis progression assessments. These techniques rely primarily on deep learning methods that enable either detection of the vertebral labels [10,15] or the corners of vertebrae from radiographs [16,17].

Other approaches to automatically estimate Cobb angle apply polynomial curves along the vertebral centroids to calculate the spinal curvature and fit a spline along the spine [18]. From this spline, perpendicular lines at each intervertebral plane level are used to calculate the maximal Cobb angle [18]. Another approach used second-order derivatives (inflection points), of the spline on vertebral labels to capture maximal curvature from ultrasound images [19], while another added a tolerance threshold to these inflection points to calculate the average curvature [20].

Automated Cobb angle measurement methods enable large-scale analysis of conditions affecting spinal alignment, and the UK Biobank imaging cohort provides a unique opportunity to assess the prevalence of degenerative scoliosis across a large and representative UK population. We employed a deep learning pipeline to segment the vertebrae bone marrow (VBM) compartments on non-dedicated Dixon MRI scans and applied a centroid-based approach to calculate the Cobb angle. Furthermore, we investigated the influence of demographic and lifestyle factors and comorbidities on Cobb angle severity.

Methods

Data

The UK Biobank recruited over 500,000 participants from across the UK, aged 40 to 85, between 2006 and 2014 [21], with a subset of 100,000 participants selected to undergo MRI

of the heart, brain, and abdomen. The UK Biobank study was approved by the North West Multi-centre Research Ethics Committee (REC reference: 11/NW/0382) with informed consent from all participants. Researchers may apply to use the UK Biobank data resource by submitting a health-related research proposal in the public interest. Additional information may be found on the UK Biobank researchers and resource catalogue pages (http://www.ukbiobank.ac.uk). Access to the fully anonymised participant data for this project was granted through the UK Biobank Application number 44584.

Image processing and MRI measurements

For this study, we utilised the abdominal neck-to-knee chemical-shift-based water-fat separation MRI, from 40,755 participants imaged between 2014-2020. Comprehensive details on the MRI abdominal protocol have been reported previously [22]. Health-related information such as demographic data, lifestyle factors, biometric measurements, and health conditions were collected during the imaging visit or from linked electronic healthcare records.

All data were processed and segmented using automated methods as previously described [23]. We manually annotated 18 VBM compartments (from the first thoracic vertebra to the first sacral vertebra) on 120 participants, which were split 80/20 between training/validation/ testing groups, respectively, to train and test the deep learning model. The Dice similarity coefficient for the 20% hold-out test group was 0.83. A cubic spline was fitted to the centroids of the VBM compartments to estimate spinal curvature. The complexity of the spline model was regulated by setting the degrees of freedom as $(n + 1) / 2$, where n is the number of VBM compartments in each dataset. Generalised cross-validation was used to optimise the parameters of the spline model. The second derivative of the fitted spline was used to identify inflection points, defined as locations where the second derivative equalled zero. Cobb angles were calculated between adjacent pairs of inflection points by measuring the angle between perpendicular lines to the spline at those locations. Additionally, to capture curvature at the boundaries of the spinal segment, Cobb angles were also computed between the terminal vertebrae and their nearest inflection points. The maximum Cobb angle was recorded as the image-derived phenotype (IDP) of interest for each participant, resulting in a single value per individual. The workflow is represented in Fig. 1.

Additional IDPs were collected from the Dixon MRI data to evaluate the interaction of muscle and fat body compartment measurements with Cobb angles from our previous work [23,24]. These IDPs included muscle compartments such as total skeletal muscle volume, thigh muscle (left and right) volume and iliopsoas (left and right) muscle volume; fat deposits such

as visceral (VAT); abdominal subcutaneous adipose tissue (ASAT) volume, and paraspinal intramuscular content, or otherwise referred to as the paraspinal proton density fat fraction (paraspinal PDFF) [23,24]. The paraspinal muscle grouping includes the erector spinae and the multifidus muscles.

Quality control

Visual quality control was performed for the 50 most extreme Cobb angles (both largest and smallest values), a random subset of 50 participants, and a subset of participants with a documented diagnosis of scoliosis in the UK Biobank and a Cobb angle < 10° of the cohort in order to identify spurious results. Any spurious VBM labels were manually corrected (Supplementary Fig. 1). No datasets were discarded due to inaccurately fitted splines.

Anthropometric factors and disease definitions

Extensive demographic, socioeconomic and biometric information was gathered during both the participant's baseline and the imaging visit through questionnaires, physical measurements and/or electronic healthcare records. Except for sex, ethnicity, Townsend deprivation index, and serum biomarkers, variables utilised in the study were taken from the imaging visit.

Ethnicity was derived from the UK Biobank field 21000 and categorised as White (any British, Irish or other white background), or Non-white, including Black (any Caribbean, African or any other Black background), Chinese, Asian (any Indian, Pakistani, Bangladeshi or any other South Asian background), and Other (mixed ethnic background and other ethnic groups). Any missing data was supplemented from the continental genetic ancestry data. Townsend deprivation index is a composite measure of socioeconomic status, composed of self-reported unemployment values, home and car ownership, and household crowding status.

Information on prior disease conditions was accessible from UK Biobank fields, which were aggregated from primary care, hospital inpatient, cancer, and death records, as well as self-reported medical questionnaires. Both International Classification of Diseases, Ninth Revision (ICD9) and International Classification of Diseases, Tenth Revision (ICD10) diagnostic codes and UK Biobank-specific fields were used to derive information regarding conditions. All conditions were binarised for the presence or absence of the condition before or on the date of the imaging visit.

Osteoporosis was identified via ICD9 and ICD10 codes from the UK Biobank fields. In addition, bone mineral density (BMD) T-score measurements were taken from the UK Biobank fields 23204, 23205, 23208, 23209, 23215, 23217, 23219, 23296, 23299, 23300, 23301 acquired via dual-energy x-ray absorptiometry at the imaging visit. These measurements were used to complete osteoporosis and osteopenia binary conditions, where osteoporosis was identified if the BMD T-scores were ≤ -2.5, and osteopenia if the BMD T-scores were > -2.5 and ≤ -1 at the lumbar spine, femur neck, femur trochanter, or femur ward areas [25].

Scoliosis

An incremental search of the UK Biobank fields listed in Supplementary Table 1 was used to identify participants with diagnosed scoliosis. Participants were reported to have childhood scoliosis according to the ICD10 coding of juvenile and idiopathic scoliosis (M41.1) or when the participants were 18 years or younger on the date of first occurrence of the condition. These participants were excluded from further analysis. Participants identified with self-reported scoliosis were derived from UK Biobank fields 131907 or 20002.

Scoliosis detected by our automated method was classified as 'scoliosis from algorithm', defined by a maximum Cobb angle greater than 10° [26]. The severity of scoliosis was categorised as follows: none (0° to 9°), mild (10° to 24°), moderate (25° to 39°), and severe (greater than 40°) [17,27].

Pain definitions

Participants at the imaging visit provided information on pain experienced in the past month, the duration of back pain and the number of falls in the past year. Healthy controls for back pain were defined as participants who had not reported experiencing back pain. Those who reported back pain were further classified into an acute cohort if the pain lasted less than three months or into a chronic cohort if the pain persisted for more than three months [28].

Study design and cohort

Dixon MRI data for 40,769 participants was acquired at the baseline imaging with data comprising imaging, health-related diagnoses and biological measurements were available. After the application of the MRI-based Cobb angle measurement algorithm, participants with missing demographic, anthropometric or health-related data such as age, ethnicity, height, Townsend deprivation index, smoking status, moderate-to-vigorous physical activity (according to metabolic equivalent task [MET] values), type 2 diabetes, back pain and leg

pain levels, osteoporosis, degenerative disc disease, VAT, ASAT, iliopsoas muscle volume and paraspinal muscle PDFF, were excluded from the study (n = 6,845). Finally, participants diagnosed with juvenile or adolescent scoliosis or who were diagnosed on or before the age of 18 were excluded to ensure subsequent associative analysis were restricted to adult-onset degenerative scoliosis (n = 21). Overall, after these exclusions, a dataset of 33,889 were included in the final analysis. An illustrative flow chart of the excluded participants can be viewed in Supplementary Fig. 2.

Statistical analysis

All summary statistics, hypothesis tests, regression models and figures were performed using R software environment version 4.3.2 for statistical computing and graphics [29]. All continuous variables were reported as mean and standard deviations (SD), and categorical variables were reported as counts and proportions of total.

To gain further insight into which variables influenced the spinal curvature in the coronal plane, Spearman correlation was performed to assess the strength of the relationship between variables of interest and the Cobb angle. Although the response variable was angular, the Cobb angles ranged from 0° to 90° and, therefore lacked periodic or cyclic properties. Consequently, the use of circular statistical approaches typically applied to angular data, was not required. As such, a linear regression analysis was used to investigate the associations between the Cobb angles and the interaction between age and sex, as well as with other IDPs, anthropometric variables and Cobb angle-related conditions. To avoid multicollinearity among covariates, the most strongly correlated with the Cobb angle were chosen from traits representing subclusters of muscle and fat volume IDP traits. The Cobb angles were log-transformed due to non-normal distribution of the data, and the covariates were standardised with units in one standard deviation and centred prior to fitting the linear regression model. The strength of the associations was expressed as standardised beta coefficients with 95% confidence intervals (CI), along with the corresponding p-values. The Bonferroni-corrected statistical significance threshold was set to 0.05/91 = 0.000549 to account for multiple tests.

Results

Abdominal MRI scans from 40,755 participants were processed, all of which had successfully fitted splines and corresponding derived Cobb angles. 6,845 participants were

excluded due to missing anthropometric variables, and 21 participants excluded due to juvenile or adolescent scoliosis diagnosis or scoliosis diagnosis attribution prior to 18 years of age. The final cohort consisted of 33,889 participants, of which 49.9% were female, with a median age of 63.86 ± 7.68 years (63.04 ± 7.48 years and 64.64 ± 7.80 for female and male participants, respectively) (Table 1).

Representative images of vertebrae masks fitted spline model and maximal Cobb angle measurement for participants without and with a scoliosis diagnosis are shown in Fig. 2.A and Fig. 2.B, respectively. The average Cobb angle for the overall cohort was 8.72 ± 5.21° (range 0.91° - 86.6°), with 9.02 ± 5.59° for female and 8.44 ± 4.79° for male participants ($p < 0.000549$). A total of 9,497 (28%) exhibited a Cobb angle above 10°, of which 53.6% were female participants (Fig. 3.A). Participants with a clinical diagnosis or self-reported scoliosis (n=170; 0.5%) had a Cobb angle ranging from 1.93° - 84.1°. Of these, 49 participants had a maximal Cobb angle below 10° (Fig. 3.B). These datasets of diagnosed scoliosis participants but with Cobb angles below 10° were visually confirmed, thus validating the algorithm's curvature estimations. Using the clinical Cobb angle threshold, scoliosis was identified in an additional 9,376 participants, 95.4% of whom were categorised as having mild scoliosis (Fig. 3.C).

Spinal curvature increased with age and was consistently higher in females compared to males (Fig. 4.A). Linear regression analysis revealed the interaction between age and sex on the Cobb angle, indicating higher Cobb angles in women compared to men regardless of age ($p < 0.000549$). The population prevalence of each scoliosis severity group was also higher in females than in males in all age groups (Fig. 4.B). To investigate the association of the spinal curvature with other anthropometric variables, separate associations were performed for the sex-stratified and severity group. Although significant, overall, the correlations to maximal Cobb angles were weak, with all variables displaying <0.25 Spearman's correlation coefficients. For both male and female participants, age ($r = 0.24$ for female, $r = 0.21$ for male, $p < 0.000549$) and paraspinal fat infiltration ($r = 0.10$ female, and $r = 0.07$ male, $p < 0.000549$) displayed the highest positive correlations to Cobb angle, whereas sitting height ($r = -0.12$ female and $r = -0.10$ male, $p < 0.000549$) and iliopsoas muscle volume indexed to height ($r = -0.09$ female, $r = -0.12$ male, $p < 0.000549$) had a negative association with spinal curvature (Fig. 5; Supplementary Table 2).

To evaluate the proportion of participants with conditions such as osteoporosis, osteopenia, back pain, leg pain and type 2 diabetes in relation to scoliosis severity, group-wise comparison of participants with and without the condition were performed. The Cobb angle was observed to be significantly higher in participants with chronic back pain compared to

those never reporting back pain or those reporting acute back pain ($p < 0.000549$; Table 2). The participants were further categorised into groups based on their Cobb angle, ranging from no scoliosis to severe scoliosis. The proportion of participants experiencing chronic back pain increased progressively with scoliosis severity. Among female participants, the prevalence increased from 12.2% in the no scoliosis group to 14.2%, 21.4% and 40.3% in the mild, moderate and severe scoliosis groups. Similarly, among male participants, the prevalence rose from 11.7% in the no scoliosis group to 14.0%, 13.4% and 21.2% in the mild, moderate and severe scoliosis groups, respectively. Additionally, significant differences were observed in Cobb angle and leg pain ($p < 0.000549$, Table 3) as well as osteoporosis ($p < 0.000549$, Table 4). No significant differences were observed between the Cobb angle severity and type two diabetes (Supplementary Table 3).

Linear regression analysis was conducted separately for female and male participants, adjusting for potential confounding factors such as age, height, smoking status, Townsend deprivation index, ethnicity, osteoporosis, degenerative disc disease, pain, and body composition IDPs to ensure a more robust evaluation of these associations. After Bonferroni correction, the regression analysis revealed that the Cobb angle was significantly and most strongly associated with age in both cohorts (female: $\beta = 0.12$ [0.11, 0.13], male: $\beta = 0.09$ [0.08, 0.10], $p < 0.000549$) (Fig. 6, Supplementary Table 4), chronic back pain (female: $\beta = 0.07$ [0.04, 0.09], male: $\beta = 0.05$ [0.03, 0.07], $p < 0.000549$), paraspinal muscle PDFF (female: $\beta = 0.08$ [0.07, 0.09], male: $\beta = 0.05$ [0.04, 0.05], $p < 0.000549$), and height ($\beta = 0.03$ [0.02, 0.04] for both sexes, $p < 0.000549$). VAT volume was negatively associated with the Cobb angle (female: $\beta = -0.06$ [-0.08, -0.05], male: $\beta = -0.07$ [-0.08, -0.05], $p < 0.000549$). Additionally, a statistically significant negative sex-specific association was observed between the Cobb angle and iliopsoas muscle volume ($\beta = -0.02$ [-0.03, -0.01], $p < 0.000549$) and a positive association with osteoporosis ($\beta = 0.04$ [0.02, 0.06], $p < 0.000549$) in male participants only. However, as the adjusted R^2 values of both models were very low, the predictors included in the models explained less than 10% of the variability in spinal curvature.

Discussion

In this study, we presented a method to automatically estimate the Cobb angle from Dixon abdominal MRI images. Since Dixon MRI allows visualisation of the VBM compartments without clear delineation of vertebral edges, we applied a centroid-based approach to

calculate the Cobb angle, providing a reliable estimate of spinal curvature despite limitations in endplate visibility. Additionally, we evaluated the prevalence of scoliosis in a middle-aged and elderly UK population sample and investigated the relationship between the Cobb angle and various anthropometric, clinical, and body composition variables, as well as conditions associated with spinal health, such as osteoporosis, chronic back pain, and degenerative disc disease, in both men and women. We applied our centroid and spline-based algorithm to estimate maximal Cobb angle for the UK Biobank imaging cohort.

As part of our quality control process for this study, we investigated any mismatch between clinical and algorithm-based assessment of scoliosis. 49 participants had a clinical diagnosis of scoliosis but a measured Cobb angle of < 10°. Visual quality control confirmed vertebrae label segmentation accuracy, spline fit and overall coronal curvature of the spine. Therefore, this discrepancy may arise from either i) previous treatment, such as physiotherapy, bracing or other methods, which may have improved spinal alignment following diagnosis, or ii) differences in Cobb angle measurements between supine and standing positions, which can influence the algorithm-based scoliosis classification. This study used scans performed in a supine position, unlike traditional scoliosis assessments conducted while standing [30]. The positional difference affects spinal curvature measurements, with Cobb angles being 7-12° lower in supine or prone positions compared to standing [7,31].

We observed a clinically diagnosed scoliosis prevalence of 0.5%, similar proportion to the previously reported prevalence of 0.8% in the UK Biobank imaging cohort [32]. However, by leveraging medical images to calculate the Cobb angle and subsequently defining scoliosis based on a Cobb angle > 10°, we identified the condition in 28% of the UK Biobank sample, greatly exceeding the diagnosed population prevalence. Moreover, the inherent reduction in the Cobb angle measurements when calculated from supine positions coupled with the traditional classification threshold of 10° suggests that our findings may still underestimate the true prevalence of scoliosis in this cohort.

Our study found that female participants had higher maximal Cobb angles, were more likely to suffer from scoliosis and exhibited accelerated Cobb angle increase with age compared to men. These findings align with previous meta-analyses that have reported a higher prevalence of scoliosis in women [5]. The sex differences have been frequently attributed to female-prevalent conditions such as osteoporosis, intervertebral disc degeneration, and smaller paraspinal or iliopsoas muscle volumes [5,33,34]. After accounting for these musculoskeletal and degenerative factors, osteoporosis remained significantly associated only in males. In males, it may indicate a more structurally impactful phenotype contributing to spinal alignment changes.

Asymmetrical mechanical loads across the spine can induce or exacerbate scoliosis by affecting vertebral bodies, intervertebral discs, and surrounding musculature. Several studies underscore the importance of torso muscle health, particularly that of the iliopsoas muscle and paraspinal muscles, on stabilising the spine - for instance, weakening of the paraspinal muscles, indicated by fat infiltration, have been associated with higher Cobb angles [28,33,35]. Zhou et. al. reported in a cohort of 50 patients with adult degenerative scoliosis that while fat infiltration measured from CT scans in all torso stabiliser muscles - multifidus, erector spinae, and psoas - showed positive associations with Cobb angle in men, women lacked an association between the fat infiltration of the psoas with the Cobb angle [35]. Our results showed a positive association of increased paraspinal fat infiltration with Cobb angle in both sexes. In contrast, iliopsoas muscle volume showed a negative association with spinal curvature in men only. These findings appear to suggest that women may rely more on other muscle groups such as the paraspinal muscle for spinal stabilisation in the coronal plane rather than the psoas muscle. Future longitudinal studies will explore the relationship between these muscle group volumes and their quality on Cobb angle progression across sexes.

In our study, both male and female participants reporting chronic back pain was higher in those with more severe spinal curvature. This association remained significant even after adjusting for known risk factors, including age, degenerative spinal conditions, iliopsoas muscle volume, and paraspinal muscle quality [4,28,36]. While spinal alignment abnormalities in both the coronal and sagittal planes are increasingly recognised as risk factors for back pain [4,37,38], our findings underscore the added importance of quantifying spinal curvature severity. The large proportion of participants without a formal scoliosis diagnosis further highlights the need to use continuous measures describing spinal curvature, such as the Cobb angle described in this paper, rather than relying solely on diagnostic labels in future studies exploring the aetiology, progression, and treatment of back pain.

Moreover, lower body weight has been associated with increased susceptibility to spinal curvature abnormalities such as kyphosis, scoliosis, and vertebral fractures, primarily attributed to lower skeletal muscle mass hampering spinal support [39]. Similarly, our results showed a negative correlation between spinal curvature and weight as well as body mass index. Whereas the presence of type two diabetes has been linked to intervertebral disc degeneration, spinal fractures as well as back pain, potentially due to the accumulation of glycation end-products that have been linked to increased collagen cross-linking, increasing vertebral frailty [40,41]. Interestingly, we did not observe differences in type two diabetes impact on the Cobb angle, yet the participants with increased VAT displayed inverse

association with Cobb angle magnitude. This was a surprising finding, which may be attributable to the biomechanics of the spine. A study on sagittal Cobb angles has shown a positive association between visceral adipose tissue and lumbar lordosis, which the authors postulated was due to the sagittal shift in the centre of gravity with increased abdominal adiposity [42,43]. The reduction of Cobb angle in the coronal plane may thus be due to the limitation of spinal twisting that is favoured toward the sagittal plane rather than the coronal, in addition to the potential enhanced structural support within the abdominal cavity that may limit the spinal movement in another plane.

It is important to note some of the limitations of the study. The MRI scans were acquired in the supine position, where the Cobb angles have been reported to be 7-12° lower compared to standing positions [7,31]. Therefore, applying a 10° threshold from supine MRI scans to define scoliosis, may underestimate its true prevalence. Furthermore, we indirectly also included BMD T-score values in the analysis by complementing the osteoporosis and osteopenia conditions by the T-score cutoffs. Despite including the variables that are typically associated with degenerative scoliosis such as age, torso muscle volumes and quality, osteoporosis and others, in the linear regression models, the models collectively accounted for less than 10% of the variability in Cobb angle in the population. Our findings also indicate that other variables may play a significant role in determining the presence and progression of scoliosis, for instance, genetic predisposition [44], biomechanical factors including shape and orientation of facet joints [33] or postural imbalance resulting in asymmetric loading on the spine [11,39]. Finally, in the UK Biobank population, distinguishing between adult de novo degenerative scoliosis and residual pre-existing adolescent idiopathic scoliosis is challenging. While we excluded participants formally diagnosed with scoliosis during adolescence, those who did not receive a timely formal diagnosis may have been inadvertently included in the undiagnosed scoliosis cohort.

Conclusions

In this study, we automatically estimated the Cobb angle from Dixon MRI images, enabling the identification of a significant proportion of participants with previously undiagnosed scoliosis and highlighting the high prevalence of the condition within the UK Biobank population. Additionally, the study highlighted sex differences in the occurrence and severity of scoliosis, the influence of paraspinal muscle quality on spinal stabilisation, and the relationship between chronic back pain and the magnitude of spinal curvature.

Declarations

Fully anonymised images and participant metadata were obtained through UK Biobank Access Application number 44584. The UK Biobank has approval from the North West Multi-Centre Research Ethics Committee (REC reference: 11/NW/0382), and obtained written informed consent from all participants before the study. All methods were performed in accordance with the relevant guidelines and regulations as presented by the appropriate authorities, including the Declaration of Helsinki.

Data Availability

Our research was conducted using UK Biobank data. Under the standard UK Biobank data sharing agreement, we (and other researchers) cannot directly share raw data obtained or derived from the UK Biobank. However, under this agreement, all of the data generated, and methodologies used in this paper are returned by us to the UK Biobank, where they will be fully available. Access is obtained directly from the UK Biobank to all bona fide researchers upon submitting a health-related research proposal to the UK Biobank https://www.ukbiobank.ac.uk.

References

1. Kelly A, Younus A, Lekgwara P. Adult degenerative scoliosis – A literature review. Interdiscip Neurosurg. 2020;20: 100661. doi:10.1016/j.inat.2019.100661

2. Smith JS, Shaffrey CI, Berven S, Glassman S, Hamill C, Horton W, et al. Operative versus nonoperative treatment of leg pain in adults with scoliosis: a retrospective review of a prospective multicenter database with two-year follow-up. Spine (Phila Pa 1976). 2009;34: 1693–1698. doi:10.1097/BRS.0b013e3181ac5fcd

3. Petrosyan E, Fares J, Lesniak MS, Koski TR, El Tecle NE. Biological principles of adult degenerative scoliosis. Trends Mol Med. 2023;29: 740–752. doi:10.1016/j.molmed.2023.05.012

4. Iwata S, Hashizume H, Yoshimura N, Oka H, Iwahashi H, Ishimoto Y, et al. Osteoporosis, spinal degenerative disorders, and their association with low back pain, activities of daily living, and physical performance in a general population. Sci Rep. 2024;14: 15860. doi:10.1038/s41598-024-64706-0

5. McAviney J, Roberts C, Sullivan B, Alevras AJ, Graham PL, Brown BT. The prevalence of adult de novo scoliosis: A systematic review and meta-analysis. Eur Spine J. 2020;29: 2960–2969. doi:10.1007/s00586-020-06453-0

6. Karpiel I, Ziębiński A, Kluszczyński M, Feige D. A survey of methods and technologies used for diagnosis of scoliosis. Sensors (Basel). 2021;21: 8410. doi:10.3390/s21248410

7. Vavruch L, Tropp H. A comparison of Cobb angle: Standing versus supine images of late-onset idiopathic scoliosis. Pol J Radiol. 2016;81: 270–276. doi:10.12659/PJR.895949

8. Wessberg P, Danielson BI, Willén J. Comparison of Cobb angles in idiopathic scoliosis on standing radiographs and supine axially loaded MRI. Spine (Phila Pa 1976). 2006;31: 3039–3044. doi:10.1097/01.brs.0000249513.91050.80

9. Asher MA, Burton DC. Adolescent idiopathic scoliosis: natural history and long term treatment effects. Scoliosis. 2006;1: 2. doi:10.1186/1748-7161-1-2

10. Horng M-H, Kuok C-P, Fu M-J, Lin C-J, Sun Y-N. Cobb angle measurement of spine from X-ray images using convolutional neural network. Comput Math Methods Med. 2019;2019: 6357171. doi:10.1155/2019/6357171

11. Kohno S, Ikeuchi M, Taniguchi S, Takemasa R, Yamamoto H, Tani T. Factors predicting progression in early degenerative lumbar scoliosis. J Orthop Surg (Hong Kong). 2011;19: 141–144. doi:10.1177/230949901101900202

12. Pritchett JW, Bortel DT. Degenerative symptomatic lumbar scoliosis. Spine (Phila Pa 1976). 1993;18: 700–703. doi:10.1097/00007632-199305000-00004

13. Gstoettner M, Sekyra K, Walochnik N, Winter P, Wachter R, Bach CM. Inter- and intraobserver reliability assessment of the Cobb angle: manual versus digital measurement tools. Eur Spine J. 2007;16: 1587–1592. doi:10.1007/s00586-007-0401-3

14. Bernstein P, Metzler J, Weinzierl M, Seifert C, Kisel W, Wacker M. Radiographic scoliosis angle estimation: spline-based measurement reveals superior reliability compared to traditional COBB method. Eur Spine J. 2021;30: 676–685.

doi:10.1007/s00586-020-06577-3

15. Chen K, Stotter C, Klestil T, Mitterer JA, Lepenik C, Nehrer S. Fully automated measurement of Cobb angles in coronal plane spine radiographs. J Clin Med. 2024;13: 4122. doi:10.3390/jcm13144122

16. Caesarendra W, Rahmaniar W, Mathew J, Thien A. Automated Cobb angle measurement for adolescent idiopathic scoliosis using convolutional neural network. Diagnostics (Basel). 2022;12: 396. doi:10.3390/diagnostics12020396

17. Rahmaniar W, Suzuki K, Lin T-L. Auto-CA: Automated Cobb angle measurement based on vertebrae detection for assessment of spinal curvature deformity. IEEE Trans Biomed Eng. 2024;71: 640–649. doi:10.1109/TBME.2023.3313126

18. Alukaev D, Kiselev S, Mustafaev T, Ainur A, Ibragimov B, Vrtovec T. A deep learning framework for vertebral morphometry and Cobb angle measurement with external validation. Eur Spine J. 2022;31: 2115–2124. doi:10.1007/s00586-022-07245-4

19. Guang-Quan Zhou, Wei-Wei Jiang, Ka-Lee Lai, Yong-Ping Zheng. Automatic measurement of spine curvature on 3-D ultrasound volume projection image with phase features. IEEE Trans Med Imaging. 2017;36: 1250–1262. doi:10.1109/TMI.2017.2674681

20. Li K, Gu H, Colglazier R, Lark R, Hubbard E, French R, et al. Deep learning automates Cobb angle measurement compared with multi-expert observers. arXiv [eess.IV]. 2024. Available: http://arxiv.org/abs/2403.12115

21. Sudlow C, Gallacher J, Allen N, Beral V, Burton P, Danesh J, et al. UK biobank: an open access resource for identifying the causes of a wide range of complex diseases of middle and old age. PLoS Med. 2015;12: e1001779. doi:10.1371/journal.pmed.1001779

22. Littlejohns TJ, Holliday J, Gibson LM, Garratt S, Oesingmann N, Alfaro-Almagro F, et al. The UK Biobank imaging enhancement of 100,000 participants: rationale, data collection, management and future directions. Nat Commun. 2020;11: 2624. doi:10.1038/s41467-020-15948-9

23. Liu Y, Basty N, Whitcher B, Bell JD, Sorokin EP, van Bruggen N, et al. Genetic architecture of 11 organ traits derived from abdominal MRI using deep learning. Elife. 2021;10. doi:10.7554/eLife.65554

24. Thanaj M, Basty N, Whitcher B, Sorokin EP, Liu Y, Srinivasan R, et al. Precision MRI

phenotyping of muscle volume and quality at a population scale. Front Physiol. 2024;15: 1288657. doi:10.3389/fphys.2024.1288657

25. Siris ES, Adler R, Bilezikian J, Bolognese M, Dawson-Hughes B, Favus MJ, et al. The clinical diagnosis of osteoporosis: a position statement from the National Bone Health Alliance Working Group. Osteoporos Int. 2014;25: 1439–1443. doi:10.1007/s00198-014-2655-z

26. Negrini S, Donzelli S, Aulisa AG, Czaprowski D, Schreiber S, de Mauroy JC, et al. 2016 SOSORT guidelines: orthopaedic and rehabilitation treatment of idiopathic scoliosis during growth. Scoliosis Spinal Disord. 2018;13: 3. doi:10.1186/s13013-017-0145-8

27. Van Goethem J, Van Campenhout A, van den Hauwe L, Parizel PM. Scoliosis. Neuroimaging Clin N Am. 2007;17: 105–115. doi:10.1016/j.nic.2006.12.001

28. Wesselink EO, Pool-Goudzwaard A, De Leener B, Law CSW, Fenyo MB, Ello GM, et al. Investigating the associations between lumbar paraspinal muscle health and age, BMI, sex, physical activity, and back pain using an automated computer-vision model: a UK Biobank study. Spine J. 2024;24: 1253–1266. doi:10.1016/j.spinee.2024.02.013

29. The R Project for Statistical Computing. [cited 18 Oct 2024]. Available: https://www.r-project.org/

30. d'Astorg H, Bourret S, Ramos-Pascual S, Szadkowski M, Le Huec J-C. Comparison of Cobb angle measurements for scoliosis assessment using different imaging modalities: a systematic review. EFORT Open Rev. 2023;8: 489–498. doi:10.1530/EOR-23-0032

31. Brink RC, Colo D, Schlösser TPC, Vincken KL, van Stralen M, Hui SCN, et al. Upright, prone, and supine spinal morphology and alignment in adolescent idiopathic scoliosis. Scoliosis Spinal Disord. 2017;12: 6. doi:10.1186/s13013-017-0111-5

32. Quintero Santofimio V, Clement A, O'Regan DP, Ware JS, McGurk KA. Identification of an increased lifetime risk of major adverse cardiovascular events in UK Biobank participants with scoliosis. Open Heart. 2023;10: e002224. doi:10.1136/openhrt-2022-002224

33. Lorbergs AL, Allaire BT, Yang L, Kiel DP, Cupples LA, Jarraya M, et al. A longitudinal study of trunk muscle properties and severity of thoracic kyphosis in women and men: The Framingham study. J Gerontol A Biol Sci Med Sci. 2019;74: 420–427. doi:10.1093/gerona/gly056

34. Kirilov N, Kirilova E, Todorov S, Nikolov N. Effect of the lumbar scoliosis on the results of dual-energy X-ray absorptiometry. Orthopedic Reviews. 2020;12: 8477. doi:10.4081/or.2020.8477

35. Zhou M, Liu L, Chen Z, Ma B, Fu X, Cheng Y, et al. Characteristics of paraspinal muscle degeneration in patients with adult degenerative scoliosis. Eur Spine J. 2023;32: 4020–4029. doi:10.1007/s00586-023-07940-w

36. Mallio CA, Russo F, Vadalà G, Papalia R, Pileri M, Mancuso V, et al. The importance of psoas muscle on low back pain: a single-center study on lumbar spine MRI. N Am Spine Soc J. 2024;18: 100326. doi:10.1016/j.xnsj.2024.100326

37. Mok FPS, Samartzis D, Karppinen J, Fong DYT, Luk KDK, Cheung KMC. Modic changes of the lumbar spine: prevalence, risk factors, and association with disc degeneration and low back pain in a large-scale population-based cohort. Spine J. 2016;16: 32–41. doi:10.1016/j.spinee.2015.09.060

38. Toyone T, Toyone T, Tanaka T, Wada Y, Kamikawa K, Ito M, et al. Changes in vertebral wedging rate between supine and standing position and its association with back pain: a prospective study in patients with osteoporotic vertebral compression fractures. Spine (Phila Pa 1976). 2006;31: 2963–2966. doi:10.1097/01.brs.0000247802.91724.7e

39. Kado DM, Huang M-H, Karlamangla AS, Cawthon P, Katzman W, Hillier TA, et al. Factors associated with kyphosis progression in older women: 15 years' experience in the study of osteoporotic fractures. J Bone Miner Res. 2013;28: 179–187. doi:10.1002/jbmr.1728

40. Viguet-Carrin S, Follet H, Gineyts E, Roux JP, Munoz F, Chapurlat R, et al. Association between collagen cross-links and trabecular microarchitecture properties of human vertebral bone. Bone. 2010;46: 342–347. doi:10.1016/j.bone.2009.10.001

41. Broz K, Walk RE, Tang SY. Complications in the spine associated with type 2 diabetes: The role of advanced glycation end-products. Med Nov Technol Devices. 2021;11: 100065. doi:10.1016/j.medntd.2021.100065

42. Wang FM, Ruby JG, Sethi A, Veras M, Telis N, Melamud E. Aging of the Spine: Characterizing genetic and physiological determinants of spinal curvature. bioRxiv. 2024. doi:10.1101/2024.02.27.24303450

43. Miranda APOC, Penha PJ, Pereira LG, Pessoa WC, João SMA. Influence of sex and

body mass index on the thoracic kyphosis and lumbar lordosis. J Manipulative Physiol Ther. 2022;45: 508–514. doi:10.1016/j.jmpt.2022.12.001

44. Stone MA, Osei-Bordom D-C, Inman RD, Sammon C, Wolber LE, Williams FMK. Heritability of spinal curvature and its relationship to disc degeneration and bone mineral density in female adult twins. Eur Spine J. 2015;24: 2387–2394. doi:10.1007/s00586-014-3477-6

Figure 1. Cobb angle measurement workflow. A - Coronal mid-slice of abdominal MRI of one participant with vertebral bone marrow labels (white) and the corresponding centroids for each compartment (red dots). B - Spline fit through the centroids (dark blue line). C - Points of inflexion derived from the second-order derivatives of the fitted spline (light blue dots). D - Cobb angles were estimated by calculating the angle between perpendicular lines to the spline at each pair of adjacent inflexion points throughout the whole spine, where the maximal Cobb angle was taken as a single measure for each participant.

Figure 2. Representative images of participants with a higher than 10 degree maximal Cobb angle with vertebrae masks and fitted spline. A - Participants without a clinical scoliosis diagnosis. B - Participants with a scoliosis diagnosis. Participants were grouped into scoliosis severity categories based on Cobb angle: mild (10-24°), moderate (25-39°), and severe (≥40°).

Figure 3. Analysis of Cobb angle by UK Biobank derived clinical scoliosis diagnosis and algorithm-based diagnosis. A - Gender specific distribution of maximal Cobb angle for participants with and without a scoliosis diagnosis code. Algorithm-based scoliosis diagnosis was assigned to participants with a maximal Cobb angle of over 10°, indicated by the dashed line. B - Confusion matrix illustrating agreement between clinical diagnosis and algorithm-based diagnosis for scoliosis. C - Proportion of participants in scoliosis categories according to diagnosis status and scoliosis severity groups. Diagnosis status combined data from hospital records, private healthcare, self-reports, and an algorithm (Cobb angle >10°), distinguishing between cases detected exclusively by the algorithm (Diagnosis - | Algorithm +), cases confirmed by both methods (Diagnosis + | Algorithm +), and cases identified only through healthcare data (Diagnosis + | Algorithm -). Participants were grouped into scoliosis

severity categories based on Cobb angle: mild (10-24°), moderate (25-39°), and severe (≥40°).

Figure 4. Relationship between Cobb angles to age and sex. A - A line plot with density plots of Cobb angles for age and sex. B - Prevalence of scoliosis by scoliosis severity group (mild - 10-24°; moderate - 25-39°; severe ≥40°) and age group, stratified by sex.

Figure 5. Sex-stratified correlation coefficients between anthropometric variables and Cobb angles. Spearman's correlation coefficient between the Cobb angle and variables of interest.

Figure 6. Sex-stratified linear regression models investigating the relationship between Cobb angles and anthropometric variables, image-derived phenotypes and conditions. Linear regression analysis derived standardised regression coefficients (beta) between log-transformed Cobb angles and standardised anthropometric variables, image-derived phenotypes and associated conditions. Colourful beta coefficient labels indicate statistically significant associations ($p < 0.000549$) after Bonferroni correction.

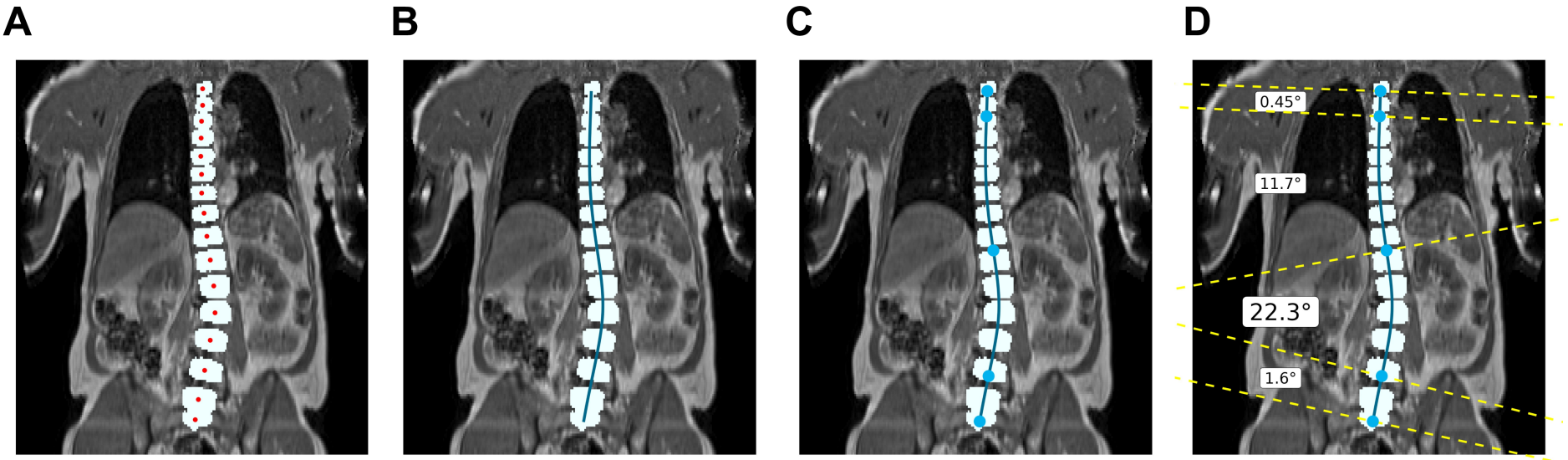
A
B
C
D
0.45°
11.7°
22.3°
1.6°

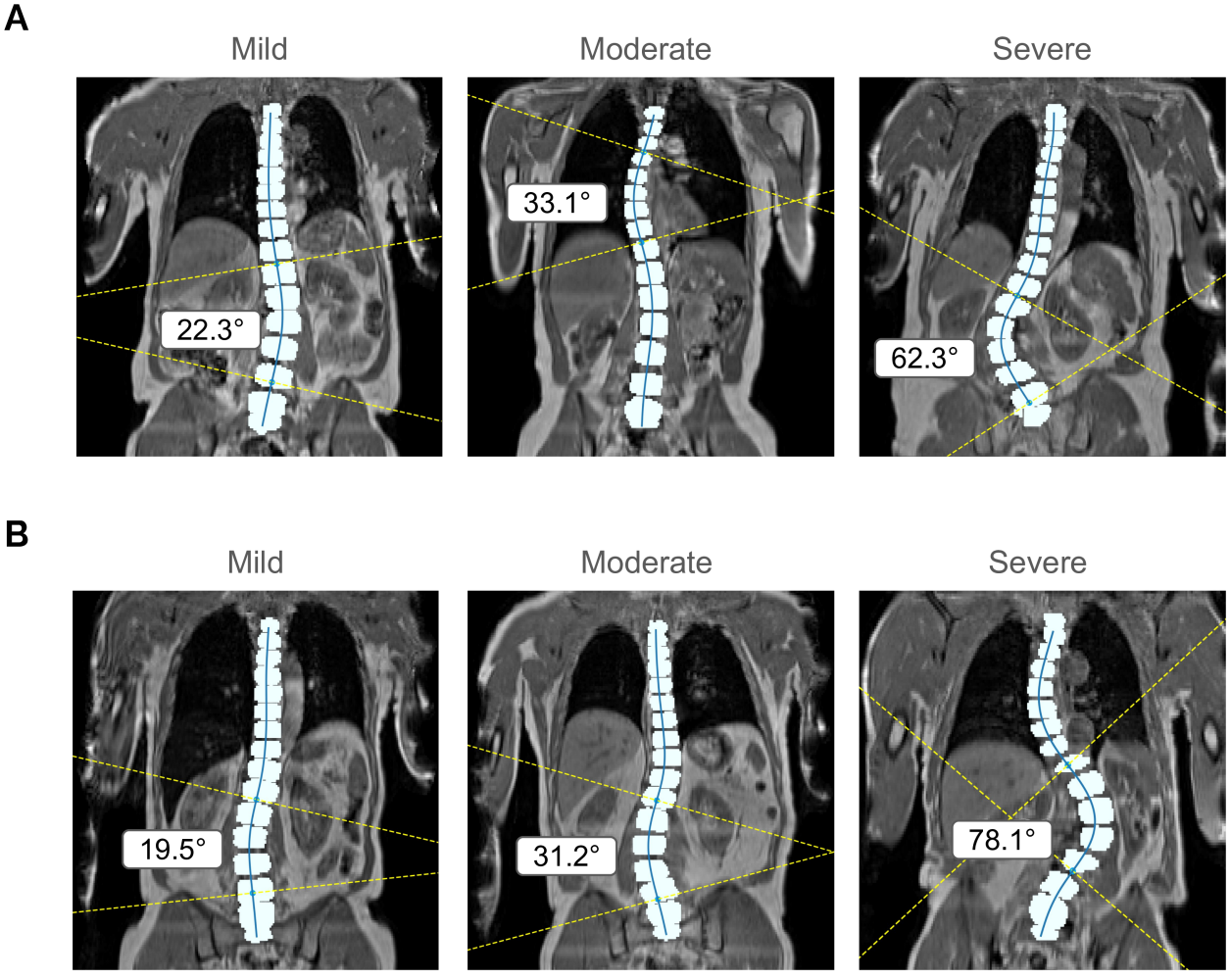
A
Mild
Moderate
Severe
22.3°
33.1°
62.3°
B
Mild
Moderate
Severe
19.5°
31.2°
78.1°

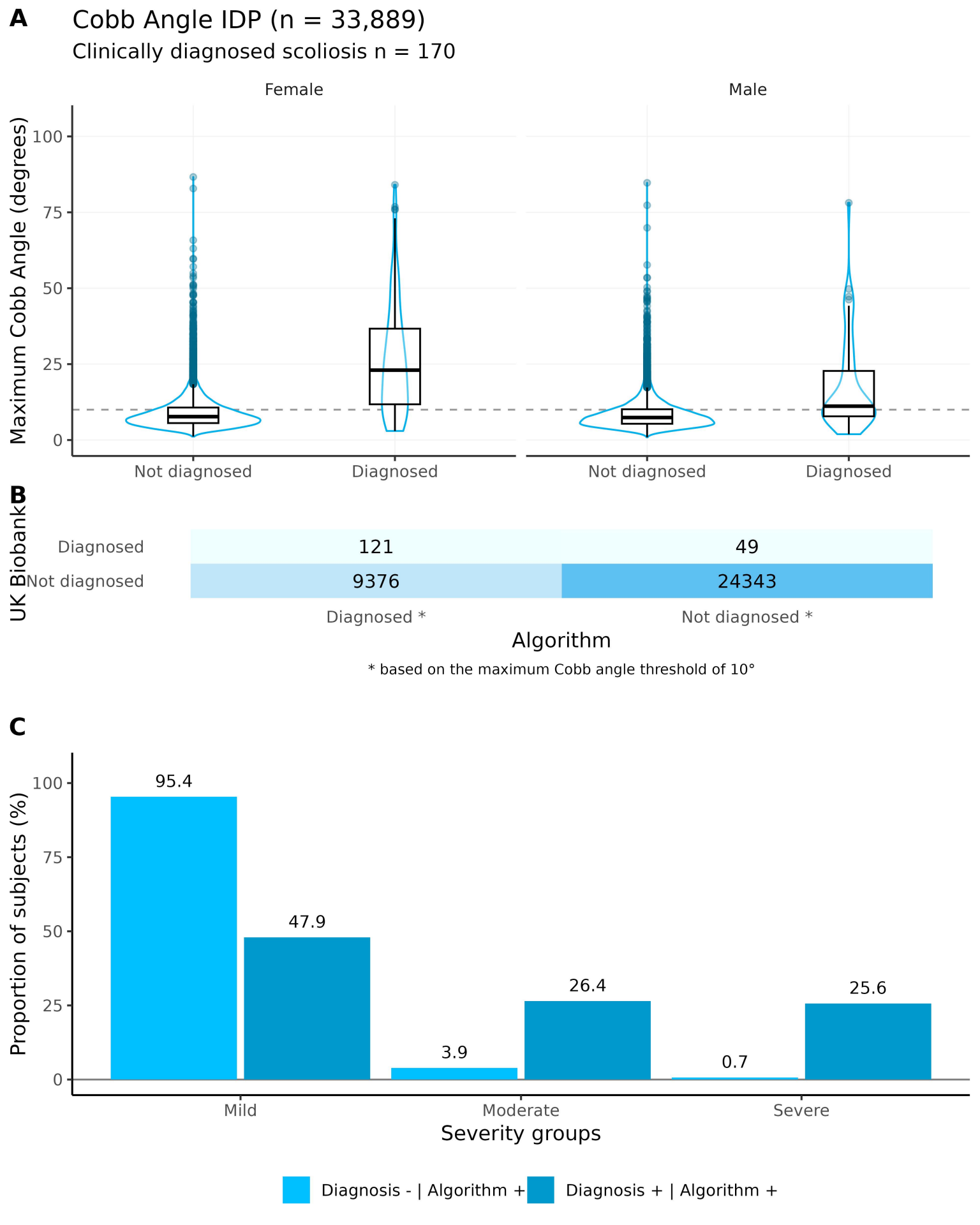
A
Cobb Angle IDP (n = 33,889)
Clinically diagnosed scoliosis n = 170
Female
Male
Maximum Cobb Angle (degrees)
100
75
50
25
0
Not diagnosed
Diagnosed
Not diagnosed
Diagnosed
B
UK Biobank
Diagnosed
Not diagnosed
121
49
9376
24343
Diagnosed *
Not diagnosed *
Algorithm
* based on the maximum Cobb angle threshold of 10°
C
Proportion of subjects (%)
100
75
50
25
0
95.4
47.9
3.9
26.4
0.7
25.6
Mild
Moderate
Severe
Severity groups
Diagnosis - | Algorithm +
Diagnosis + | Algorithm +

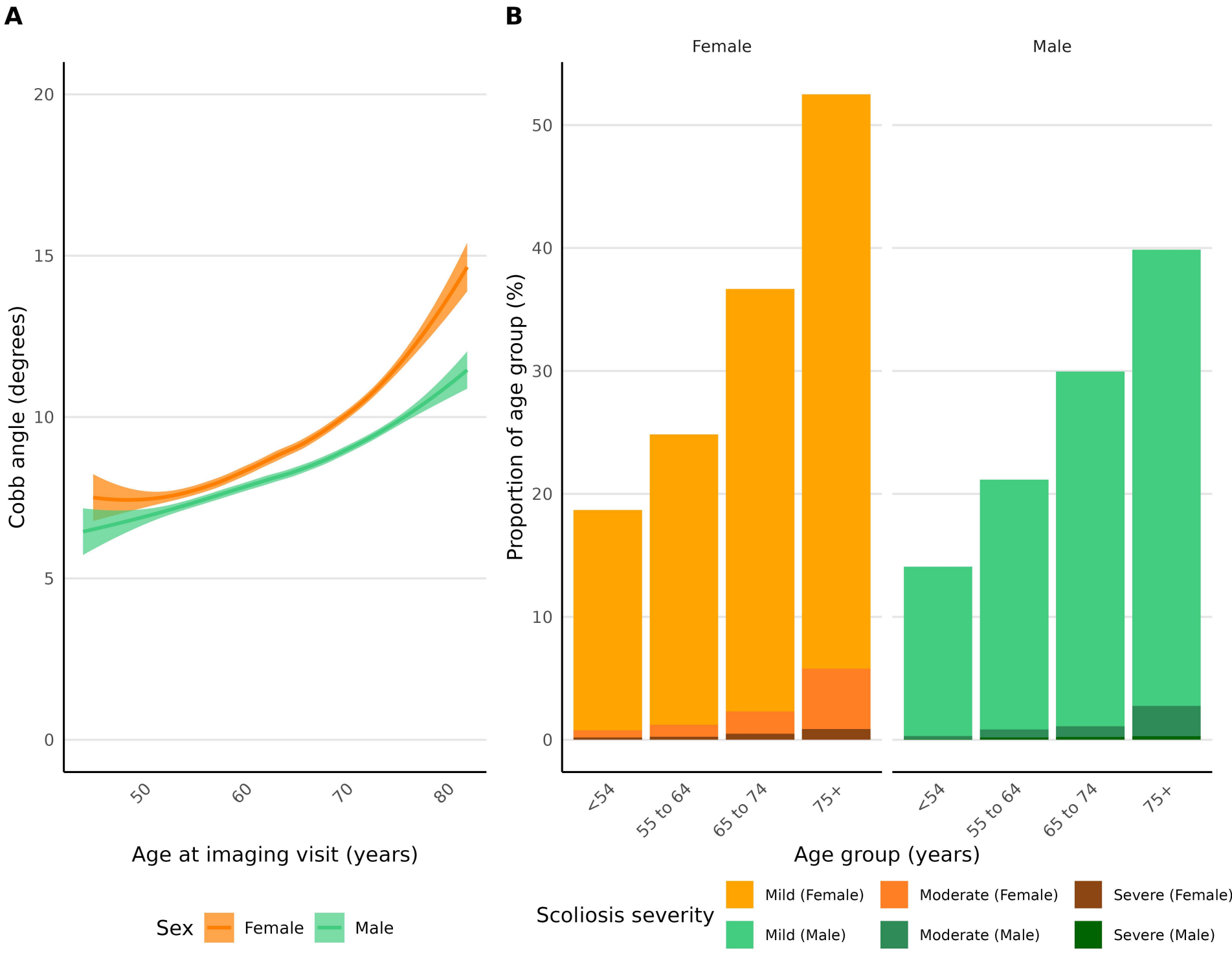
A
Cobb angle (degrees)
20
15
10
5
0
50
60
70
80
Age at imaging visit (years)
Sex
Female
Male
B
Female
Male
Proportion of age group (%)
50
40
30
20
10
0
<54
55 to 64
65 to 74
75+
Age group (years)
Scoliosis severity
Mild (Female)
Moderate (Female)
Severe (Female)
Mild (Male)
Moderate (Male)
Severe (Male)

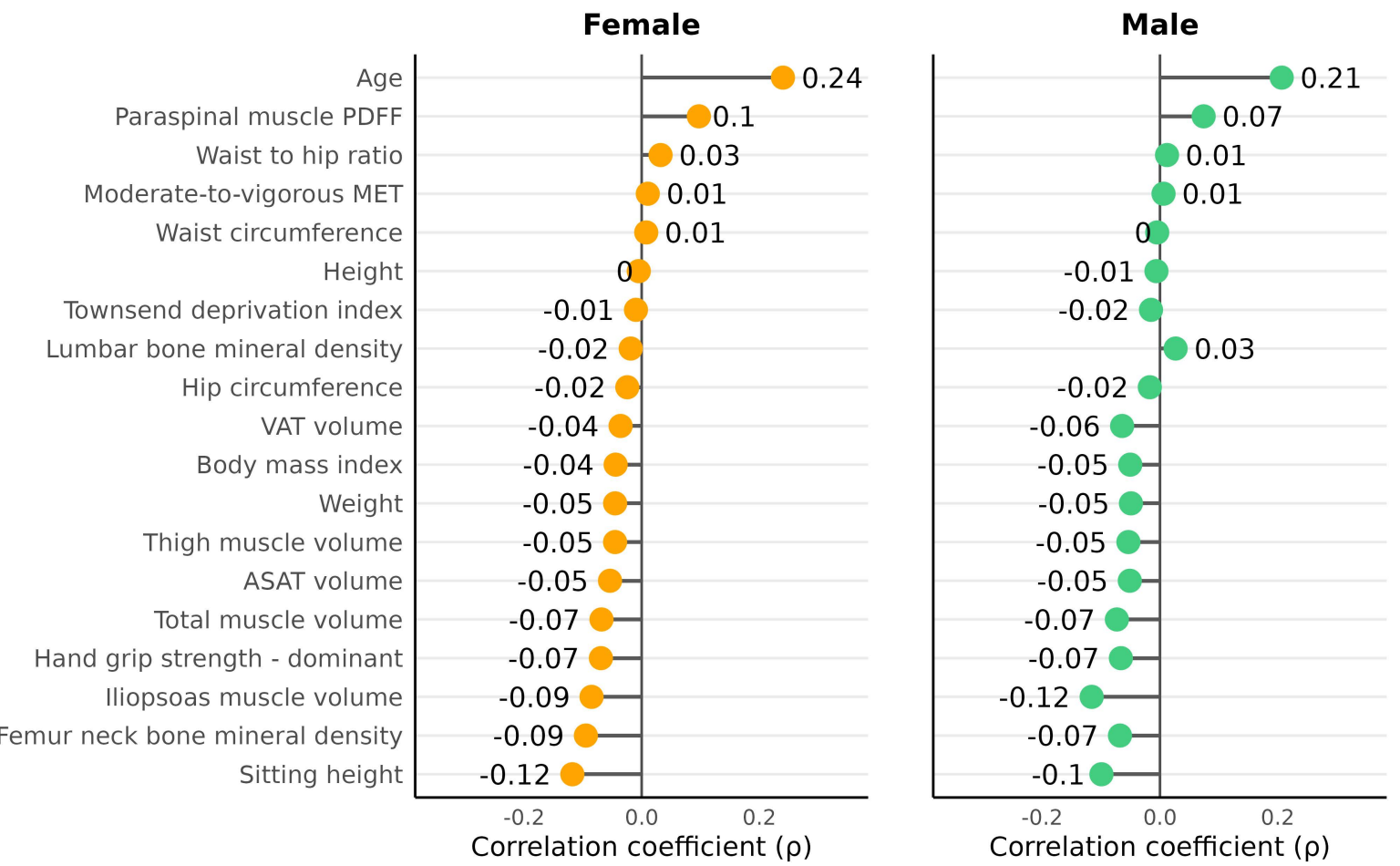
Female
Male
Age
Paraspinal muscle PDFF
Waist to hip ratio
Moderate-to-vigorous MET
Waist circumference
Height
Townsend deprivation index
Lumbar bone mineral density
Hip circumference
VAT volume
Body mass index
Weight
Thigh muscle volume
ASAT volume
Total muscle volume
Hand grip strength - dominant
Iliopsoas muscle volume
Femur neck bone mineral density
Sitting height
0.24
0.1
0.03
0.01
0.01
0
-0.01
-0.02
-0.02
-0.04
-0.04
-0.05
-0.05
-0.05
-0.07
-0.07
-0.09
-0.09
-0.12
0.21
0.07
0.01
0.01
0
-0.01
-0.02
0.03
-0.02
-0.06
-0.05
-0.05
-0.05
-0.05
-0.07
-0.07
-0.12
-0.07
-0.1
-0.2
0.0
0.2
Correlation coefficient (ρ)
-0.2
0.0
0.2
Correlation coefficient (ρ)

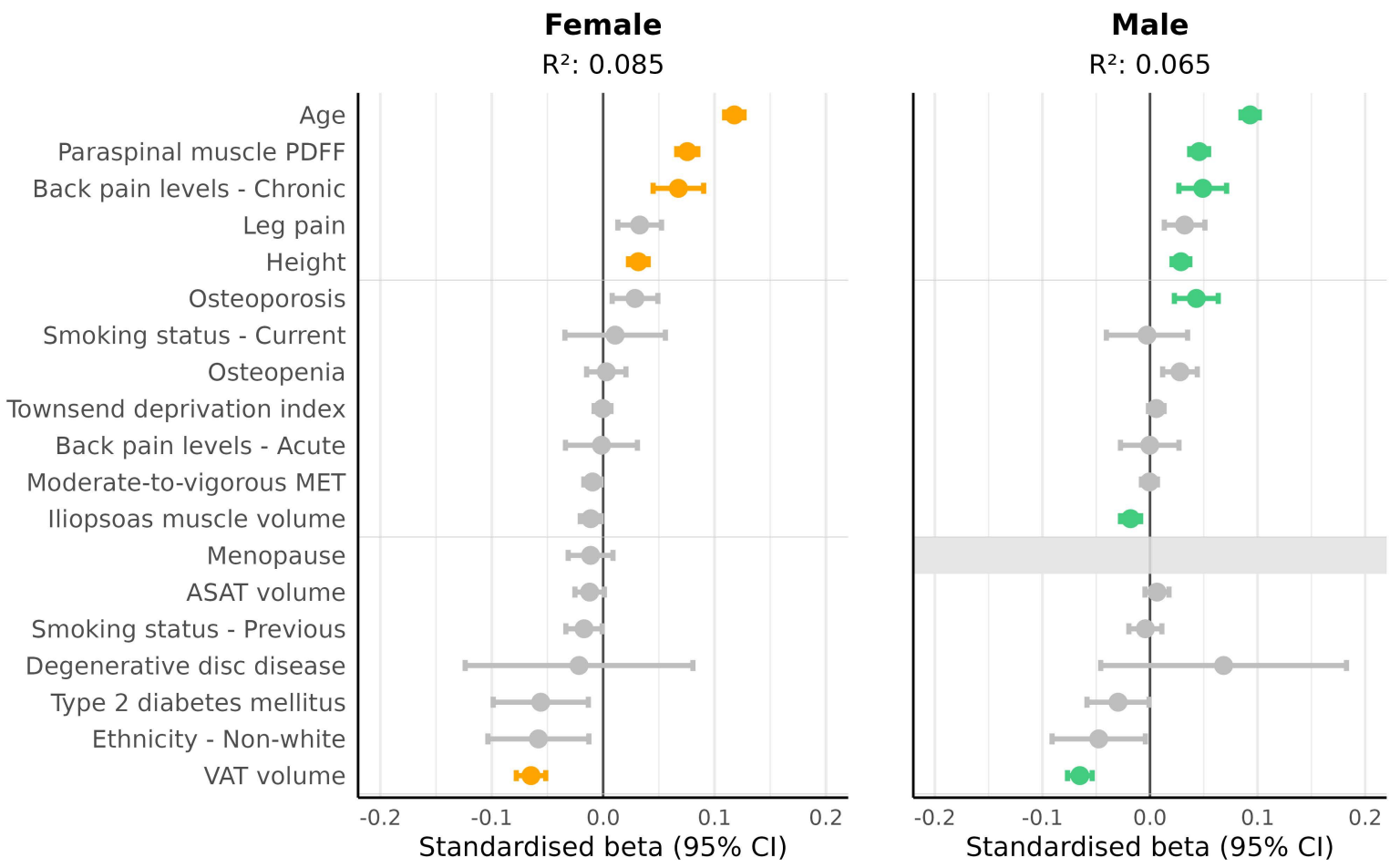
Female
R²: 0.085
Male
R²: 0.065
Age
Paraspinal muscle PDFF
Back pain levels - Chronic
Leg pain
Height
Osteoporosis
Smoking status - Current
Osteopenia
Townsend deprivation index
Back pain levels - Acute
Moderate-to-vigorous MET
Iliopsoas muscle volume
Menopause
ASAT volume
Smoking status - Previous
Degenerative disc disease
Type 2 diabetes mellitus
Ethnicity - Non-white
VAT volume
-0.2
-0.1
0.0
0.1
0.2
Standardised beta (95% CI)
-0.2
-0.1
0.0
0.1
0.2
Standardised beta (95% CI)

Tables

Variable	Overall n = 33,889[1]	Female n = 16,907[1]	Male n = 16,982[1]
Anthropometric			
Ethnicity			
White	32,908 (97%)	16,423 (97%)	16,485 (97%)
Non-white	981 (2.9%)	484 (2.9%)	497 (2.9%)
Age (years)	63.85 ± 7.68	63.04 ± 7.48	64.64 ± 7.80
Townsend deprivation index	-1.90 ± 2.72	-1.83 ± 2.72	-1.96 ± 2.71
Height (cm)	169.56 ± 9.23	162.91 ± 6.22	176.18 ± 6.61
Weight (kg)	76.23 ± 15.07	68.77 ± 12.98	83.65 ± 13.22
Body mass index (kg/m²)	26.42 ± 4.32	25.91 ± 4.69	26.93 ± 3.85
Waist circumference (cm)	88.36 ± 12.62	82.45 ± 11.70	94.22 ± 10.60
Hip circumference (cm)	100.65 ± 8.61	100.63 ± 9.76	100.66 ± 7.30
Waist to hip ratio	0.88 ± 0.09	0.82 ± 0.07	0.93 ± 0.06
Hang grip strength - dominant (kg)	31.75 ± 10.56	24.31 ± 5.99	39.09 ± 8.80
Moderate-to-vigorous MET (hours/week)	19.43 ± 13.58	19.17 ± 13.40	19.68 ± 13.75
Smoking status			
Never	21,170 (62%)	11,150 (66%)	10,020 (59%)
Previous	11,575 (34%)	5,269 (31%)	6,306 (37%)
Current	1,144 (3.4%)	488 (2.9%)	656 (3.9%)
Alcohol status			
Never	1,045 (3.1%)	669 (4.0%)	376 (2.2%)
Current	31,729 (94%)	15,668 (93%)	16,061 (95%)
Previous	1,107 (3.3%)	568 (3.4%)	539 (3.2%)
Femur neck BMD (T-score)	-0.67 ± 1.05	-0.72 ± 1.08	-0.63 ± 1.03
Lumbar BMD (T-score)	-0.08 ± 1.62	-0.52 ± 1.49	0.35 ± 1.62
Image derived			
Abdominal subcutaneous adipose tissue volume (L)	8.36 ± 4.07	9.74 ± 4.36	7.00 ± 3.24
Visceral adipose tissue volume (L)	3.96 ± 2.31	2.77 ± 1.56	5.15 ± 2.33
Total muscle volume (L)	18.00 ± 4.63	14.10 ± 1.95	21.88 ± 2.99
Iliopsoas muscle volume (L)	0.65 ± 0.17	0.51 ± 0.08	0.79 ± 0.12
Thigh muscle volume (L)	8.56 ± 2.24	6.72 ± 1.00	10.38 ± 1.51
Paraspinal muscle PDFF (%)	7.27 ± 3.79	7.73 ± 3.97	6.81 ± 3.54
Conditions			

Back pain levels			
Never	27,358 (81%)	13,755 (81%)	13,603 (80%)
Acute	2,245 (6.6%)	958 (5.7%)	1,287 (7.6%)
Chronic	4,286 (13%)	2,194 (13%)	2,092 (12%)
Leg pain	6,333 (19%)	3,197 (19%)	3,136 (18%)
Type 2 diabetes mellitus	1,745 (5.1%)	554 (3.3%)	1,191 (7.0%)
Osteoporosis	7,923 (23%)	4,540 (27%)	3,383 (20%)
Osteopenia	14,420 (43%)	7,004 (41%)	7,416 (44%)
Degenerative disc disease	157 (0.5%)	90 (0.5%)	67 (0.4%)
Diagnosed scoliosis [2]	170 (0.5%)	113 (0.7%)	57 (0.3%)
Cobb angle (°)	8.72 ± 5.21	9.02 ± 5.59	8.44 ± 4.79
Subjects with Cobb angle above 10°	9,497 (28%)	5,086 (30%)	4,411 (26%)
Severity range			
None	24,392 (72%)	11,821 (70%)	12,571 (74%)
Mild	9,005 (27%)	4,776 (28%)	4,229 (25%)
Moderate	397 (1.2%)	248 (1.5%)	149 (0.9%)
Severe	95 (0.3%)	62 (0.4%)	33 (0.2%)

[1] Categorical - count (proportion, %); Continuous - mean ± standard deviation

[2] From hospital admission, primary care sources and self-reported data

Table 1. Study population demographic characteristics, separated by gender. Values are reported as means with standard deviations for continuous variables, and counts with proportion of total population for overall, female and male cohorts for categorical variables. BMD - bone mineral density; MET - metabolically equivalent task; PDFF - proton density fat fraction.

	Female				**Male**			
	Never	**Acute**	**Chronic**	**ANOVA**	**Never**	**Acute**	**Chronic**	**ANOVA**
Count (n)	13,755	958	2,194		13,603	1,287	2,092	
Cobb angle (°)	8.9 ± 5.3	8.6 ± 4.97	10.0 ± 7.4 **	<0.001	8.4 ± 4.7	8.2 ± 4.8	8.9 ± 5.2 **	<0.001

Table 2. Cobb angle comparison for female and male participants with back pain. Significance was first tested by one-way ANOVA, and if significant, further post-hoc Tukey test. * indicate statistically significant for $p < 0.05$, ** indicate statistically significant after Bonferroni correction.

	Female		Male	
	No leg pain	**Leg pain**	**No leg pain**	**Leg pain**
Count (n)	13,710	3,197	13,846	3,136
Cobb angle (°)	8.9 ± 5.5	9.5 ± 6.1 **	8.4 ± 4.7	8.7 ± 5.0 **

Table 3. Cobb angle comparison for female and male participants with leg pain. Significance was first tested by Wilcox rank-sum test, and further adjusted by Bonferroni correction. * indicate statistically significant associations ($p < 0.05$), ** indicate statistically significant after Bonferroni correction ($p < 0.000549$).

	Female				Male			
	None	**Osteopenia**	**Osteoporosis**	**ANOVA**	**None**	**Osteopenia**	**Osteoporosis**	**ANOVA**
Count (n)	5,363	7,004	4,540		6,183	7,416	3,383	
Cobb angle (°)	8.7 ± 5.2	8.8 ± 5.4	9.7 ± 6.2 **	<0.001	8.2 ± 4.4	8.4 ± 4.7 *	9.0 ± 5.4 **	<0.001

Table 4. Cobb angle comparison for female and male participants with osteoporosis and osteopenia. Significance was first tested by one-way ANOVA, and if significant, further post-hoc Tukey test. * indicate statistically significant associations ($p < 0.05$), ** indicate statistically significant after Bonferroni correction ($p < 0.000549$).